scientific reports

OPEN

Activation of the Hepcidin-Ferroportin1 pathway in the brain and astrocytic–neuronal crosstalk to counteract iron dyshomeostasis during aging

Mariarosa Mezzanotte[1], Giorgia Ammirata[1,3], Marina Boido[2], Serena Stanga[2,4✉] & Antonella Roetto[1,4✉]

During physiological aging, iron accumulates in the brain with a preferential distribution in regions that are more vulnerable to age-dependent neurodegeneration such as the cerebral cortex and hippocampus. In the brain of aged wild-type mice, alteration of the Brain Blood Barrier integrity, together with a marked inflammatory and oxidative state lead to increased permeability and deregulation of brain-iron homeostasis. In this context, we found that iron accumulation drives Hepcidin upregulation in the brain and the inhibition of the iron exporter Ferroportin1. We also observed the transcription and the increase of NCOA4 levels in the aged brain together with the increase of light-chain enriched ferritin heteropolymers, more efficient as iron chelators. Interestingly, in cerebral cortex and hippocampus, Ferroportin1 is mainly expressed by astrocytes, while the iron storage protein ferritin light-chain by neurons. This differential distribution suggests that astrocytes mediate iron shuttling in the nervous tissue and that neurons are unable to metabolize it. Our findings highlight for the first time that Hepcidin/Ferroportin1 axis and NCOA4 are directly involved in iron metabolism in mice brain during physiological aging as a response to a higher brain iron influx.

Iron is essential in many cellular and biological processes but it can also generate Reactive Oxidative Species (ROS) by Fenton reaction, contributing to the pathophysiology of many diseases[1]. Iron homeostasis is guaranteed by the action of proteins involved in iron import: Transferrin (Tf), Transferrin Receptors (TfR1), and Divalent Metal Transporter 1 (DMT1); iron export: Ferroportin 1 (Fpn1)[2] and iron storage: cytosolic ferritin (Ft) heteropolymer, composed of 24 subunits of ferritin heavy (Ft-H) and light (Ft-L) chains[3]. However, the regulator of iron content and availability in the body is Hepcidin (Hepc), a peptide mainly produced by hepatocytes, that regulates iron levels by interacting with Fpn1. When body iron increases, Hepc rises as well and this causes Fpn1 degradation and, consequently, iron retention by the cells. So, Hepc lowers the amount of iron in the serum[1], controlling intestinal iron uptake and release from splenic macrophages[4], according to the body's needs. The opposite situation occurs in iron deficiency conditions (i.e. anemia, hypoxia, ineffective erythropoiesis)[4,5].

A new protein involved in iron metabolism is the Nuclear Receptor Coactivator 4 (NCOA4), a cargo protein able to promote selective autophagic ferritin degradation[6]. After NCOA4 binding to Ft-H, ferritin is carried to the lysosome and degraded and iron is released in the cytoplasm, modulating intracellular iron regulation, via "ferritinophagy"[7]. NCOA4 levels are in turn regulated by intracellular iron status[7] and by the interaction with HERC2, an E3 ubiquitin-protein ligase[7,8]. In a NCOA4 knockout mouse model, it has been shown an iron phenotype with increased levels of Tf saturation, serum Ft and liver Hepc and an increase of Ft deposits in the

[1]Department of Clinical and Biological Sciences, University of Turin, Turin, Italy. [2]Neuroscience Institute Cavalieri Ottolenghi, Department of Neuroscience Rita Levi Montalcini, University of Turin, Turin, Italy. [3]Present address: Molecular Biotechnology Center Guido Tarone, University of Turin, Turin, Italy. [4]These authors contributed equally: Serena Stanga and Antonella Roetto. ✉email: serena.stanga@unito.it; antonella.roetto@unito.it

liver and spleen[9]. Recently, an extra-hepatic function of NCOA4 was demonstrated[10]. However, up to now, no data are available on brain NCOA4 and Hepc/Fpn1 expression and function during aging or neurodegeneration.

In the brain, iron regulates important functions such as neurotransmission, myelination and division of neuronal cells[11]. Iron reaches the brain crossing the Blood Brain Barrier (BBB)[12]. Iron up-take is then mediated by TfR1 expressed on the luminal side of brain capillaries[13]. Once inside the cell, iron is released into the cytoplasmic space and exported through the abluminal membrane by unknown mechanisms in which Fpn1 and other transporters may be involved[14].

It has been shown that Hepc is present in the brain, in mature astrocytes and oligodendrocytes[15], where it plays a role in the control of iron amount together with its own iron regulatory proteins[14]. However, it is not yet clear whether the Hepc acting on Fpn1 in the brain is the one produced in the liver or not[15]. Although the peptide size and its amphipathic cationic structure[16] would allow hepatic Hepc to pass the BBB, it has been shown that there is an endogenous cerebral Hepc expression[17] and that it responds to brain iron state[18].

Several conditions which are typical of aging such as inflammation, BBB damage due to the release of inflammatory mediators, free radicals and vascular endothelial growth factor[19] cause iron redistribution and unbalance in the brain[20].

With age, iron accumulates in the cerebral cortex (Ctx) and in the hippocampus (Hip), regions which are involved in neurodegenerative disorders[12], but the underlying mechanism it is not yet known.

Here we demonstrated that NCOA4, Hepc and Fpn1 are activated in WT mice brain during physiological aging as a consequence of iron accumulation and that they participate to brain response to increased iron entry. Furthermore, we assessed the astrocytic–neuronal crosstalk and we found that the iron exporter Fpn1 co-localizes with astrocytes, while neurons are enriched in the iron deposit Ft-L heteropolymers, both in the Ctx and Hip. These data suggest that, while glial cells enhance iron export in the nervous tissue, neurons accumulate it, triggering neurodegenerative processes.

Results

Iron amount and distribution in the brain during aging correlates to the level of BBB permeability.
Brain Iron Content (BIC) increases during aging at each experimental time point (Fig. 1A) in different brain areas as shown by histochemical analysis with DAB-enhanced Prussian blue Perls' staining (Fig. 1B). WT O mice show an increased number of brown precipitates compared to WT A mice in specific parenchymal region such as Ctx, Hip CA regions, third ventricle (3 V) and striatum. Similarly, we also observed an age-dependent increase in the levels of iron in liver and in serum of old mice indicating a general perturbation of iron metabolism with physiological aging (Supplementary Figure 1S). Since progressive BBB damage is occurring not only in neurodegeneration[21] but also during aging, we analysed Zonula occludens-1 (ZO-1) protein, whose role is to maintain the compactness of BBB acting as a bridge connecting Claudin and Occludin proteins to the actin cytoskeleton in order to stabilize the tight junction (TJ) structure[22]. ZO-1 levels significantly decrease during aging (Fig. 1C), therefore, we can hypothesize that age-dependent BBB altered permeability, could contribute, together with age-dependent metal dyshomeostasis, to iron accumulation in specific areas of the brain during physiological aging.

Increased inflammatory and oxidative stress state during brain aging.
The two main markers of neuroinflammation and oxidative stress, Serum amyloid A1 (SAA1) [23] and Nuclear factor erythroid 2-related factor 2 (Nrf2) [24], are overexpressed in aged brains. SAA1 expression levels is more than 20 times higher in WT O animals compared to WT A (Fig. 2A) and Nrf2 expression levels are constantly increasing during aging (Fig. 2B).

Moreover, we performed immunohistochemistry to selectively label reactive intermediate filament protein (GFAP)-positive astrocytes. In fact, GFAP is an indicator of neuroinflammation in the CNS[25] and it is also involved in the progression of neurodegeneration in ischemia, AD, MS, Amyotrophic Lateral Sclerosis (ALS) and PD[26–28]. In addition, we also checked the expression of the Ionized calcium-binding adaptor molecule 1 (IBA-1), a microglia/macrophage-specific calcium-binding protein which is also a key molecule in proinflammatory processes[29]. We identified high astrocytes activation and an increased expression of microglia in both parenchymal regions of WT O mice where iron accumulated, Ctx and Hip, compared to those of WT A (Fig. 2C and D).

These data show that iron accumulation in the brain is accompanied by the neuroinflammatory and antioxidative stress response.

Hepc/Fpn1 activation and ferritins response to iron accumulation during brain aging.
In order to evaluate if the Hepc/Fpn1 axis has a role during brain physiologic aging, we measured both Hepc and Fpn1 in the whole brain of aged mice. Interestingly, we observed that Hepc gene expression significantly increases in WT M-A and WT O mice brain (Fig. 3A), while Fpn1 protein decreases (Fig. 3B). To investigate how neuronal cells responded to the increase of iron amount, we analysed in the total brain also the iron deposit protein ferritins (Ft) and separately evaluating the two polymers: ferritin light-chains (Ft-L) and ferritin heavy-chains (Ft-H). As expected, we observed a significant increase in Ft-L amount (Fig. 3C), but, surprisingly a 40% reduction of Ft-H in WT O animals' brains compared to the WT A (Fig. 3D). We also checked for NCOA4 levels of transcription and translation in the brain. NCOA4 gene results to be highly transcribed in the brain and its expression is comparable to that of the liver (Ct values 25 ± 1 and 24 ± 1.5 respectively) (Fig. 3E and[9]).

Furthermore, NCOA4 protein amount is also significantly increased in WT O mice brain compared to WT A (Fig. 3F).

Altogether, these results demonstrate that in old mice brain iron accumulation together with the inflammatory condition (Fig. 2A–C and D) induces Hepc expression and, consequently, Fpn1 degradation; therefore, activation
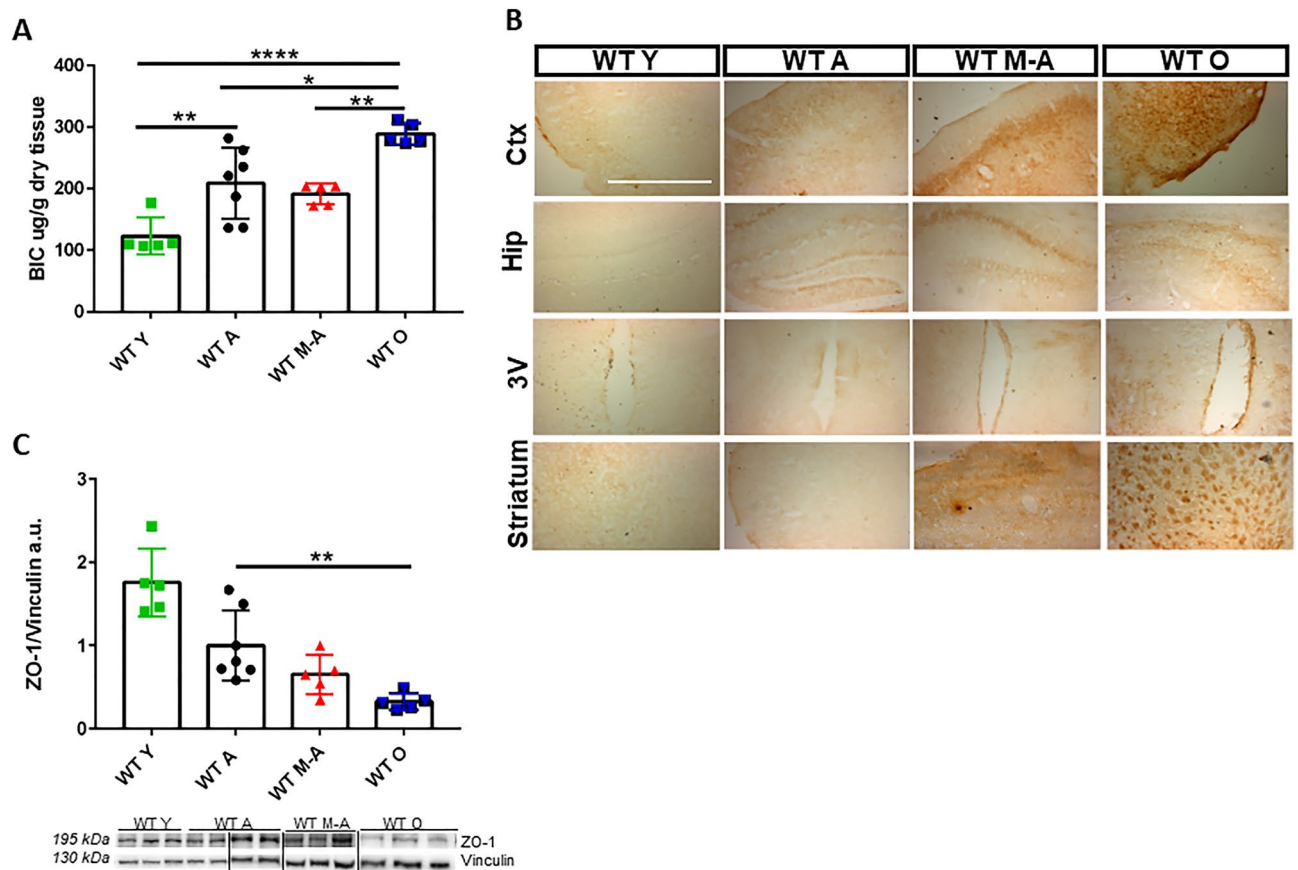
Figure 1. Iron accumulation in WT mice brain and impaired permeability of blood brain barrier (BBB). (**A**) Brain Iron Content (BIC) from mice total brain at different ages. (**B**) Sections of mice brain stained with DAB-enhanced Prussian Blue staining in cerebral cortex (Ctx), hippocampus (Hip), third ventricle (3v) and Striatum during aging. Scale bars:10X. Results on Liver Iron Content (LIC), Prussian Blue staining and serum iron are shown in Supplementary Figure 1S. (**C**) Western blotting analysis and quantification of ZO-1. Vertical black lines indicate image taken from different gels. Full length ZO-1 blot with a positive control (HeLa cells) is shown in Supplementary Figure 3S. *Statistically significant vs WT A control group *$P < 0.05$; **$P < 0.01$ ***$P < 0.001$ using two-tailed Student's t-test. Number of analyzed mice: WT Y n = 5, WT A n = 7, WT M-A n = 5 and WT O n = 5.

of the Hepc/Fpn1 pathway in the brain promotes cellular iron retention. Furthermore, our results show for the first time that NCOA4 is transcribed in the brain and that it increases in WT O mice.

Cellular distribution of iron deposits and export proteins in Ctx and Hip.

We decided to further analyse Fpn1 localization in mice brains. Immunofluorescence experiments revealed that Fpn1 is localized mainly in the Ctx and Hip at each age (Fig. 4A). Moreover, we checked for the cellular distribution of Fpn1 within the nervous tissue. When we co-labelled Fpn1 with specific astrocytic and neuronal markers, Glutamate Transporter (GLAST) and Vesicular Glutamate Transporter 1 (VGLUT1) respectively, we found that Fpn1 co-localizes with astrocytes (Fig. 4B).

Additionally, to discriminate if the accumulation of iron occurred specifically inside neurons and/or astrocytes, we co-stained Ft-L and Ft-H with Microtubule-Associated Protein 2 (MAP2) and GFAP, respectively. Compared to WT A, in WT O mice brains we observed a specific and marked increase of Ft-L deposits in cortical and hippocampal neurons but not in astrocytes (Fig. 4C). Ft-H isoform was also identified in the soma of cortical and hippocampal neurons (Fig. 4D), and resulted to be less abundant than Ft-L isoform in these cells. These results demonstrate that there is an "iron cross-talk" between astrocytes and neurons but they are participating differently in the process of iron distribution and metabolism/accumulation.

Discussion

During aging and in neurodegenerative diseases with old age onset such as PD and AD, an increase in iron content was observed in multiple brain regions[30,31]. In pathological conditions, it was demonstrated to be the cause of motor deterioration[12] and of proteins aggregation[32] leading to cellular stress[33]. Parallel to deposition of iron in the brain, in the periphery, systemic iron levels decrease and old subjects are subjected to anemia[34].
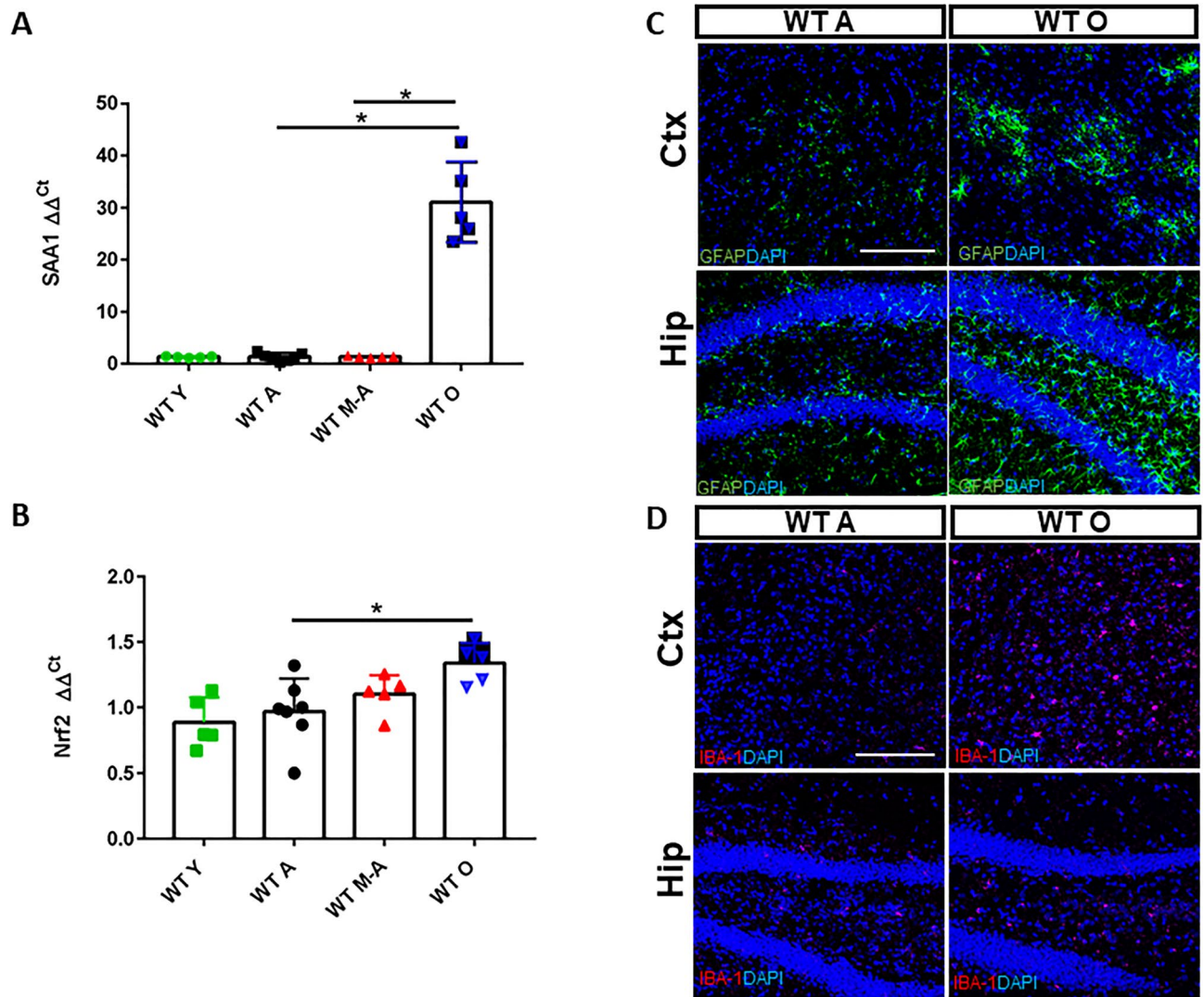
Figure 2. Iron-dependent inflammatory response and oxidative stress during aging. (**A**) Real-time PCR of SAA1 in total brain from all genotypes. (**B**) Nrf2 mRNA expression levels in total brain. The expression levels of the two genes were normalized to levels of β-glucuronidase (Gus-β) housekeeping gene (material and methods section). (**C**) Immunofluorescence anti-GFAP (green) and anti-IBA1 (pink) antibodies in cerebral cortex (Ctx) and hippocampus (Hip); 4,6-diamidino-2-phenylindole (DAPI) (blue) was used to counterstain cell nuclei. Scale bars:40X. *Statistically significant vs WT A control group *$P < 0.05$; **$P < 0.01$ ***$P < 0.001$ using OneWay ANOVA followed by Bonferroni's post hoc analysis. Number of analyzed mice: (**A**–**B**): WT Y n = 5, WT A n = 7, WT M-A n = 5 and WT O n = 5; (**C**–**D**): WT A n = 5 and WT O n = 5.

Systemic iron regulation is based on a complex protein regulatory system in which the hepatic Hepcidin (Hepc) plays a major role. Indeed, the iron dependent modulation of Hepc expression determines de facto iron availability in the body[35]. In the brain, iron homeostasis is regulated by the same proteins network that acts at the systemic level[30] and the Hepc regulatory system is active also in the CNS[31]. Indeed, Hepc is expressed by glial cells and neurons from different brain regions and, under brain iron accumulation, it is activated and it induces Fpn1 decrease[36,37]. However, it is not clear yet whether this rely on brain or hepatic Hepc[15]. Moreover, it is not known how this regulatory system respond to intracerebral iron increase during aging. Intrigued by this question, we studied the brain expression of proteins involved in systemic iron homeostasis in wild type (WT) mice during aging.

We characterized the state of the brain at different ages by studying BBB integrity, brain inflammation and oxidative state, all key features related to the process of aging and that influence iron homeostasis (Figs. 1 and 2). It is known that BBB mitigates iron entry from the blood to the brain through highly regulated and selective systems: iron crosses the BBB bound to Tf through TfR-mediated endocytosis[38] and brain vascular endothelial cells (BVECs) export intracellular iron using Fpn1, whose activity is conditioned by the iron ferroxidases ceruloplasmin and hephaestin[31]. Finally, iron is acquired by nervous cells through iron transporter proteins, as DMT1, and released from these cells through Fpn1[31].
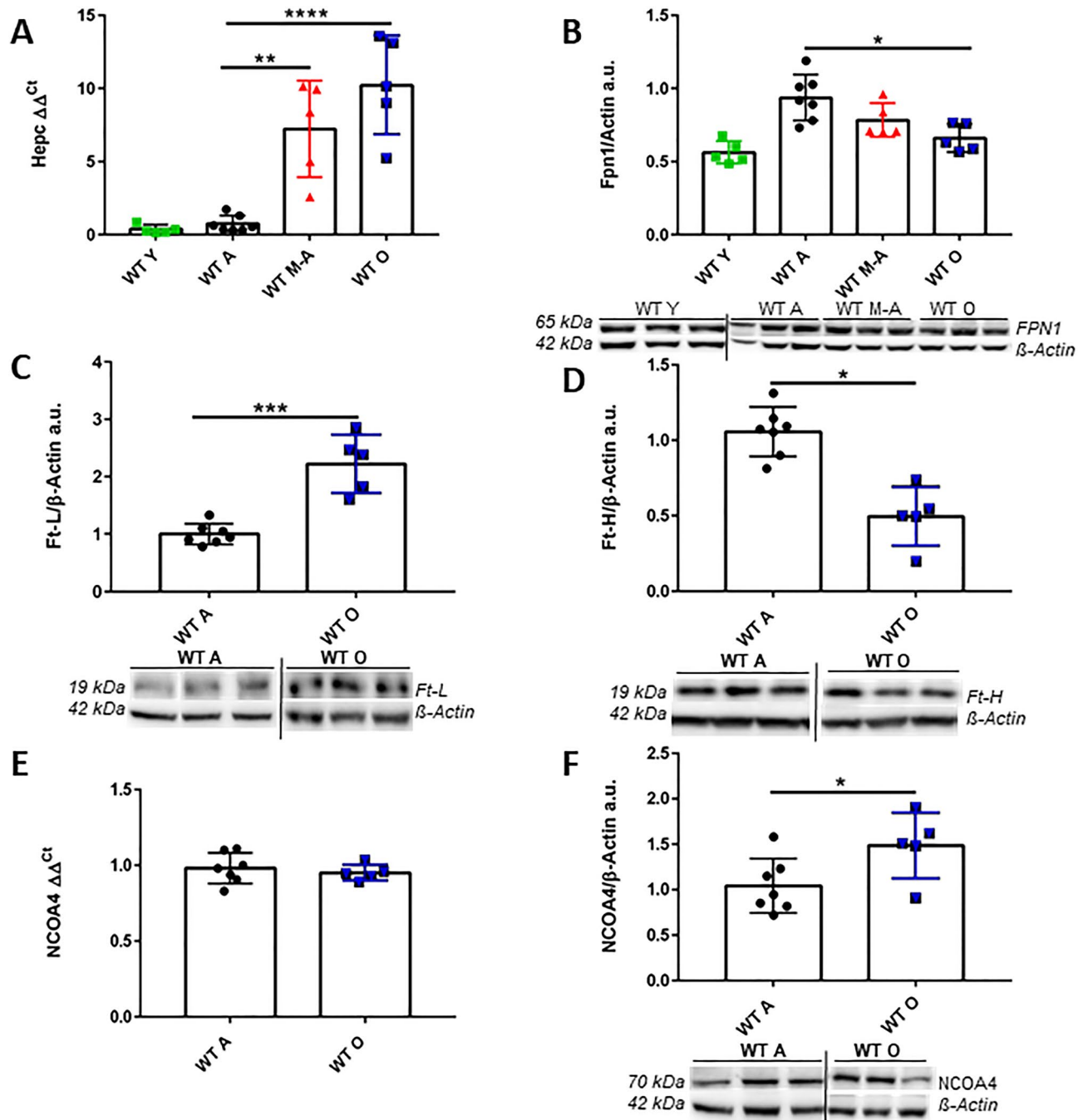
Figure 3. Hepcidin expression and iron transport/storage proteins quantification in mice brain. (**A**) Hepc transcription pattern. (**B**) Western blotting analysis and quantification of Fpn1. (**C**) Ft-L and (**D**) Ft-H. in mice total brain. (**E**) Real-time PCR of NCOA4 in total brain. The expression levels of NCOA4 were normalized to the levels of β-Glucuronidase (Gus-β) housekeeping gene (material and methods section) and (**F**) Western blotting analysis and quantification of NCOA4. Vertical black lines in blots images indicate that they are taken from different gels. Full length blots are presented in Supplementary Figure 4S. The full length blot with a positive control (liver) for Fpn1 is presented in Supplementary Figure 5S. *Statistically significant vs WT A control group *$P < 0.05$; **$P < 0.01$ ***$P < 0.001$ using OneWay ANOVA followed by Bonferroni's post hoc analysis or two-tailed Student's t-test. Number of analyzed mice: WT Y n = 5, WT A n = 7, WT M-A n = 5 and WT O n = 5.

It is also known that iron accumulation in the brain, triggers the release of pro-inflammatory cytokines, determining an environment prone to neurodegeneration[39].
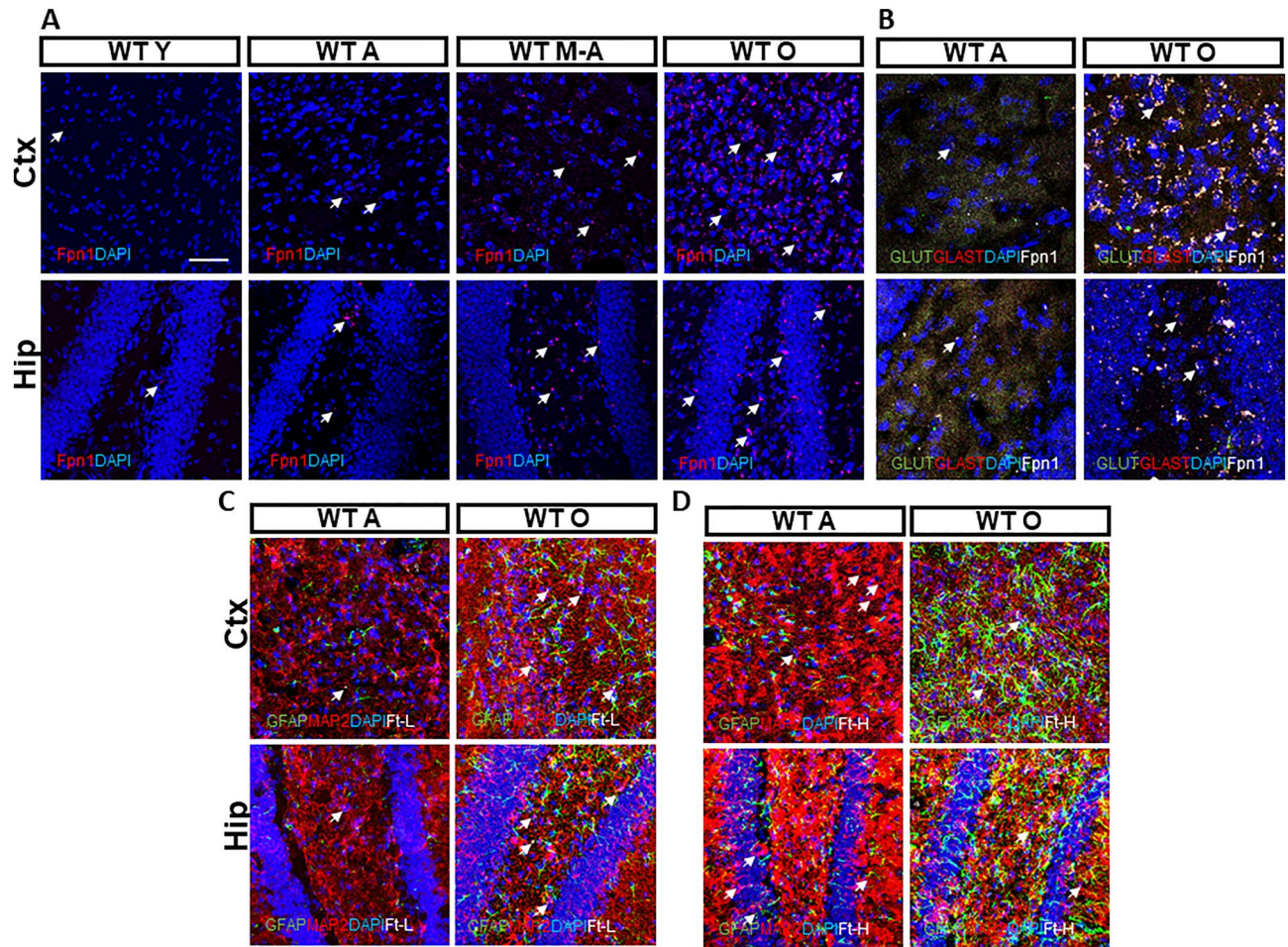
Figure 4. Ferroportin 1, Ferritin L and H chain protein cellular allocation in Ctx and Hip. (**A**) Immunofluorescence anti-Fpn1 antibody (red) in cerebral cortex (Ctx) and hippocampus (Hip). (**B**) Immunofluorescence of neuronal and astrocytic cells using anti-GLUT1 (green), anti-GLAST (red) and anti-Fpn1 antibodies in cerebral cortex (Ctx) and hippocampus (Hip). (**C, D**) Immunofluorescence of astrocytic and neuronal cells using anti-GFAP (green), anti-MAP2 (red), anti-Ft-L and anti-Ft-H antibodies in cerebral cortex (Ctx) and hippocampus (Hip). 4,6-diamidino-2-phenylindole (DAPI) (blue) was used to counterstain cell nuclei. Scale bars: 63X. Number of analyzed mice: WT Y n = 5, WT A n = 5, WT M-A n = 5 and WT O n = 5. Specifically, neuronal (MAP2) and Ferritins (Ft-L and Ft-H) localization are shown in Supplementary Figure 6S.

Indeed, we demonstrated the progressive accumulation of iron during physiological aging in the Ctx, Hip, third ventricle and striatum and the parallel decrease of the BBB integrity. As a consequence of iron accumulation, the transcription of SAA-1, a protein related to acute inflammation and marker of neuroinflammation[40,41], described also in AD as able to stimulate the release of cytokines and chemokines[23,41], increases up to 1000 times in old mice brain. Moreover, the transcription of Nrf2, a redox-sensitive transcription factor[24], is also increased, supporting the evidence of a stressful condition in WT O mice brain.

During aging, a consistent activation of astrocytes and a generalized neuroinflammation are evident[42]. In line with these findings, in both Ctx and Hip of WT O mice we observed high astrocytic and microglial activation.

Interestingly, in this context of increased iron deposition and inflammation in the brain, we found the activation of the Hepc/Fpn1 pathway: brain Hepc transcription increases and brain Fpn1 amount gradually decreases during aging. These observations are in line with what Sato and colleagues observed in the cerebral cortex and in mitochondria isolated from the brain of aged mice[43]. To better decipher the mechanism of the regulation of iron content in neuronal tissue during physiological aging, we also analyzed the iron deposit protein Ft and a newly characterized protein, NCOA4, since it is involved in Ft degradation and its inactivation in mice causes iron accumulation in the liver[9]. Specifically, NCOA4 promotes autophagic ferritin degradation through its binding to Ft-H subunit[7,44]. Ferritin levels are enhanced in a cellular model (HeLa cells) in which NCOA4 is silenced, suggesting that ferritin is constantly degraded by an NCOA4-dependent pathway[45]. Moreover, when NCOA4 knockdown is selectively targeting hepatocytes, the protein silencing promotes an increase in both iron amount and ferritin levels[46].

Surprisingly, in old mice's brains we found an increased amount of NCOA4, contrary to what happens in the liver[9]. Furthermore, specifically evaluating the ferritin polymers, we observed an increase of Ft-L and a decrease of Ft-H chains in the aged mice brains. These data demonstrated that a differential Ft chains degradation occurs
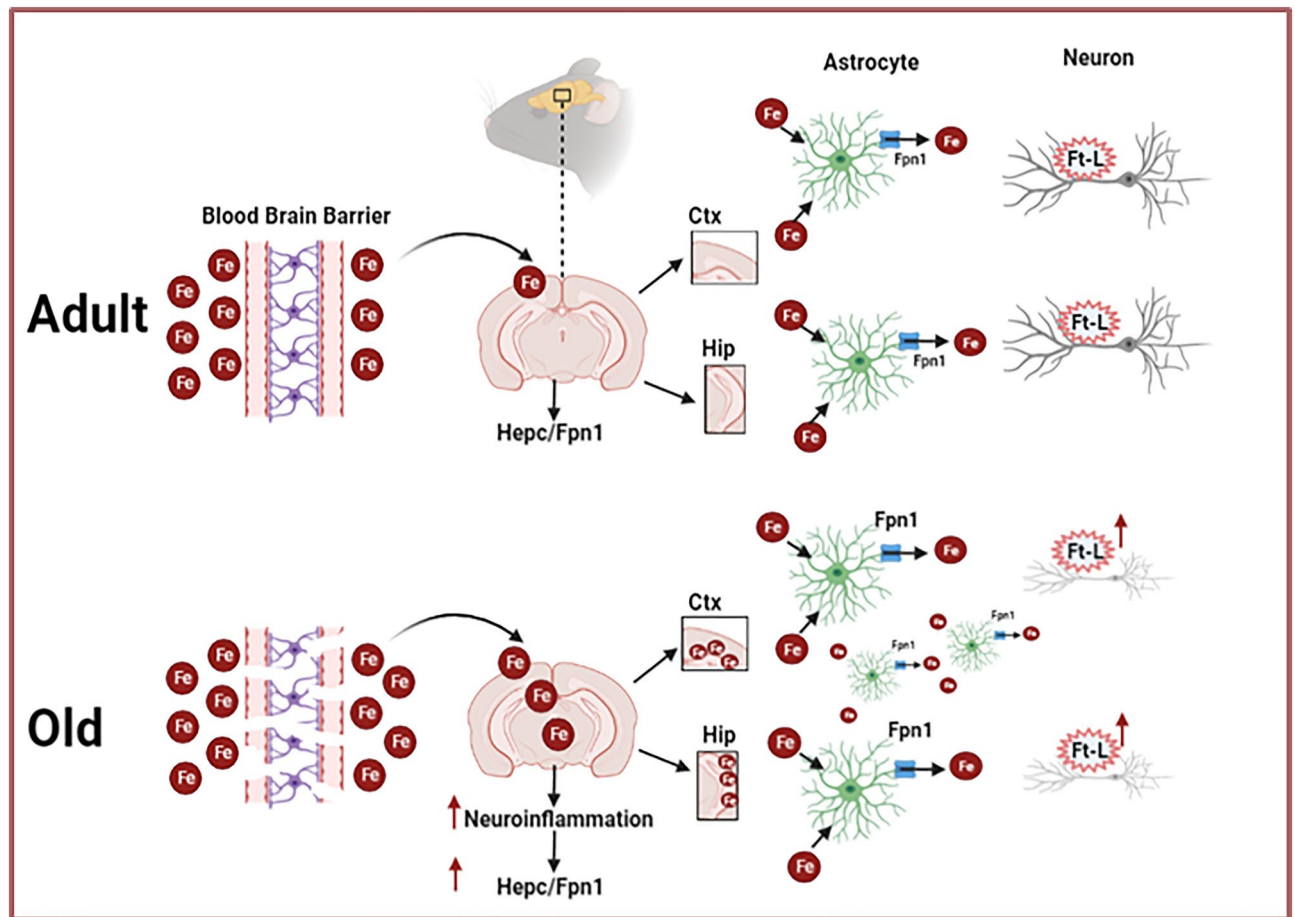
Figure 5. Iron regulation in the brain during aging. Schematic representation illustrating iron metabolism in old mice brains vs adults (see text for details). Fe: iron; Hepc: Hepcidin; Fpn1: Ferroportin 1; Ft-L: Ferritin-L; Ctx: cerebral cortex; Hip: hippocampus.

in both cortical and hippocampal neurons of old animals. We can suppose that Ft-L enriched heteropolymers are more efficient in iron chelation[3] and are also more abundant in cortical and hippocampal neurons.

Interestingly, when we analysed Fpn1 localization in the brain by immunofluorescence, we found that Fpn1 colocalized with astrocytes, both in the Ctx and Hip. On the contrary, Ferritin accumulated in cortical and hippocampal neurons close to the soma, but not in astrocytes. We suggest that this could be due to a different detoxifying mechanism carried out by neurons and astrocytes, aimed either to store or remove iron excess, respectively. On the whole, this data revealed that aging dependent brain iron accumulation compromises the cells specific response: astrocytes, which are less susceptible than neurons to iron deposits-related toxicity[47] and which play a protective role towards neurons[42], have an increased iron export, while, neurons increase the metal storage in Ft-L rich heteropolymers. These deposits could trigger the neuronal death in Ctx and Hip evidenced during aging and even more during neurodegeneration[30].

Furthermore, we showed for the first time that NCOA4 is transcribed in brain cells and that its expression is increased in WT O animals brain.

In conclusion, we demonstrated that even during physiologic aging, iron accumulates in the brain and that its accumulation, selectively localized in the Ctx and Hip, triggers neuroinflammation and the modification of the Hepc/Fpn1 pathway, all this enhancing iron availability imbalance and oxidative stress that could lead to neurodegeneration (Fig. 5).

In perspective, since NDs are characterized by inappropriate Hepc production[48], a therapeutic approach aimed at modifying the Hepc response could be taken in consideration. Different strategies could be used, such as mini-Hepc and Hepc agonists[49,50] by the stimulation/inhibition of Hepc production by targeting its regulators[35,48,51–53]. Additional research studies in animal models of NDs are required to clarify the CNS response to the increased iron aimed to exploit the results for the prevention and clinical management of patients with these diseases.

Methods

Animals. C57BL/6 J mice (WT) used for the study were purchased from the Jackson Laboratory and subdivided for age according to its classification (https://www.jax.org): until 2 months of age mice are considered Young (WT Y n = 5); from 2 to 6 months of age Adult (WT A n = 7); from 6 to 12 months of age Middle-aged (WT M-A n = 5) and from 12 months of age (between 18–24 months of age) Old (WT O n = 5) (Table 1S). Since

from a pilot analysis on potential gender-related issues, no gender bias was observed (Supplementary Figure 2S), both male and female mice were analysed and grouped according to their age. Mice were housed in polycarbonate cages (Tecnoplast, Buggirate, Italy) provided with sawdust bedding, boxes/tunnels hideout as environmental enrichment. Food and water were provided ad libitum; environmental conditions were 12 h/12 h light/dark cycle, room temperature 24 °C ± 1 °C and room humidity 55% ± 5%. Each group of mice was fed with a Standard Diet (SD) (VRF1, Special Diets Services, Essex, United Kingdom). Mice were anaesthetized (ketamine, 100 mg/kg; Ketavet, Bayern, Leverkusen, Germany; xylazine, 5 mg/kg; Rompun; Bayer, Milan, Italy) and sacrificed by cervical dislocation. To performed histological analysis, a subset of at least n = 5 WT A and WT O mice were transcardially perfused with 4% paraformaldehyde (PFA) in phosphate buffered saline (PBS). Animals housing and all the experimental procedures were performed in accordance with European (Official Journal of the European Union L276 del 20/10/2010, Vol. 53, p. 33–80) and National Legislation (Gazzetta Ufficiale n° 61 del 14/03/2014, p. 2–68) for the protection of animals used for scientific purposes and the experimental procedure was approved by the Ethical Committee of the University of Turin and conducted according the ARRIVE guidelines.

Real-time quantitative PCR.   Total RNA from whole brain was extracted with TRIzol reagent. For reverse transcription, 2 µg of total RNA, 25 µM random hexamers and 100 U of reverse transcriptase (Applied Biosystems, California, USA) were used. Gene expression levels were measured using Real-time quantitative PCR in a CFX96 Real-time System (Bio-Rad, California, USA). For Nuclear factor erythroid 2-related factor 2 (Nfr2) and NCOA4 gene analysis, SYBR Green PCR technology (EVAGreen, Bio-Rad, California, USA) was used with specific primers (Supplementary Table 2S). For Hepc and Serum Amyloid A1 (SAA1) genes analysis, Taqman PCR method was used (Assays-on-Demand, Gene Expression Products, Applied Biosystems, California, USA). β-glucuronidase (Gus-β) was used as housekeeping control. Real-time quantitative PCR of the animals' transcripts was carried out making duplicates of each n (n per group = min 3). The results were analyzed using the ΔΔCt method[54].

Immunoblotting.   The Fpn1, Ft-H, Ft-L, NCOA4 and Zonula occludens-1 (ZO-1) proteins' amount in the whole brain homogenates was evaluated by Western Blotting using specific antibodies. 50 µg of total brain lysates were separated on 6–12% SDS polyacrylamide gel and immunoblotted[55]. Primary antibodies Fpn1 (G-16), β-Actin (C-4), NCOA4 or ARA 70 (H-300) (Santa Cruz Biotechnology, Dallas, Texas, USA), ZO-1 (GeneTex, California, USA) and Vinculin (Invitrogen, Massachusetts, USA) were used. Antibodies used to detect Ft-H and Ft-L were provided by Sonia Levi, University of Vita Salute, Milan, Italy. Data were normalized on β-Actin or Vinculin amount in the same samples (Image Lab 4.0.1 Software, Bio-Rad, California, USA)[56]. Complete reference to all the antibodies is reported in Supplementary List 1.

Immunofluorescence.   Animals were perfused, brains were removed, post-fixed in PFA for 24 h at 4 °C and cryoprotected in 30% sucrose in 0.12 M phosphate buffer[57]. Brains were cut in 30 µm thick coronal sections collected in PBS and then stained to detect: Fpn1 (G-16, Santa Cruz Biotechnology, Dallas, Texas, USA), Ft-L, Ft-H (S. Levi, University of Vita Salute, Milan), Glial Fibrillary Acidic Protein (GFAP) (Dako, California, United States), Microtubule-Associated Protein 2 (MAP2) (Merck Millipore Burlington, Massachusetts, United States), Vesicular Glutamate Transporter 1 (VGLUT1) (Merck Millipore Burlington, Massachusetts, United States), Glutamate Transporter (GLAST) (Thermo Fischer Scientific Waltham, Massachusetts, United States) and Ionized calcium-binding adaptor molecule 1 (IBA-1) (Abcam, Cambridge, United Kingdom). After overnight incubation at 4 °C in PBS with 2% normal donkey serum (NDS)[58], sections were exposed to Cy2-, Cy3- (Jackson ImmunoResearch Laboratories, West Grove, PA) and 647 Alexa Fluor-conjugated secondary antibodies (Molecular Probes Inc, Eugene Oregon) for 1 h at room temperature. DAPI (4,6-diamidino-2-phenylindole, Fluka, Italy) was used to counterstain cell nuclei. After processing, sections were mounted with Tris-glycerol supplemented with 10% Mowiol (Calbiochem, LaJolla, CA). The samples were examined by a Leica TCS SP5 confocal laser scanning microscope (Leica, Mannheim); z-stacks images were taken at 40X and 63X magnification.

Iron parameters.   Brain nonheme iron content (BIC) was evaluated using 20 mg of dissected and dried murine whole brains[59]. Perfused brains were stained for nonheme ferrous iron by Prussian blue Perl's using a commercial kit (Bio-Optica, Milan, Italy). To improve the sensitivity, an intensification step with DAB (3-3′-diaminobenzidine tetrahydrochloride)[60] was performed. Images were taken at 10X magnification using a Leica DM4000B automated microscope with IM50 program for acquisition (Leica Microsystems, Wetzlar, Germany).

Statistical analysis.   One-way ANOVA followed by Bonferroni's post hoc analysis or two-tailed Student's t-test were applied according to the experimental group's number. P values of < 0.05 were considered as statistically significant. Analyses were performed with Image Lab 4.0.1 and GraphPad Prism 7.00. Data were expressed as average ± SD of the mean. Significance was defined as *$P < 0.05$, **$P < 0.01$ and ***$P < 0.001$. WT adult (A) mice were used as normalizer. The number of samples in each experimental condition is indicated in the figure legends. In each Western Blotting experiment, we reported 3 samples per group.

Data availability
The data regarding reference genes for Nrf2, NCOA4 and Gus-B primers are openly available in the repository "Nucleotide" at https://www.ncbi.nlm.nih.gov/nuccore, reference numbers NM_010902.4, NM_019744.4 and NM_010368.2.

References

1. Ganz, T. Systemic iron homeostasis. *Physiol. Rev.* **93**, 1721–1741. https://doi.org/10.1152/physrev.00008.2013 (2013).
2. Ginzburg, Y. Z. Hepcidin-ferroportin axis in health and disease. *Vitam. Horm.* **110**, 17–45. https://doi.org/10.1016/bs.vh.2019.01.002 (2019).
3. Arosio, P., Ingrassia, R. & Cavadini, P. Ferritins: a family of molecules for iron storage, antioxidation and more. *Biochem. Biophys. Acta.* **1790**, 589–599. https://doi.org/10.1016/j.bbagen.2008.09.004 (2009).
4. Sangkhae, V. & Nemeth, E. Regulation of the iron homeostatic hormone hepcidin. *Adv. Nutr. (Bethesda, Md.)* **8**, 126–136. https://doi.org/10.3945/an.116.013961 (2017).
5. Roetto, A., Mezzanotte, M. & Pellegrino, R. M. The functional versatility of transferrin receptor 2 and its therapeutic value. *Pharmaceuticals (Basel)* https://doi.org/10.3390/ph11040115 (2018).
6. Mancias, J. D., Wang, X., Gygi, S. P., Harper, J. W. & Kimmelman, A. C. Quantitative proteomics identifies NCOA4 as the cargo receptor mediating ferritinophagy. *Nature* **509**, 105–109. https://doi.org/10.1038/nature13148 (2014).
7. Mancias, J. D. *et al.* Ferritinophagy via NCOA4 is required for erythropoiesis and is regulated by iron dependent HERC2-mediated proteolysis. *Elife* https://doi.org/10.7554/eLife.10308 (2015).
8. Quiles Del Rey, M. & Mancias, J. D. NCOA4-mediated ferritinophagy: a potential link to neurodegeneration. *Front. Neurosci.* **13**, 238. https://doi.org/10.3389/fnins.2019.00238 (2019).
9. Bellelli, R. *et al.* NCOA4 deficiency impairs systemic iron homeostasis. *Cell Rep.* **14**, 411–421. https://doi.org/10.1016/j.celrep.2015.12.065 (2016).
10. Nai, A. *et al.* NCOA4-mediated ferritinophagy in macrophages is crucial to sustain erythropoiesis in mice. *Haematologica* **106**, 795–805. https://doi.org/10.3324/haematol.2019.241232 (2021).
11. Moos, T., Nielsen, T. R., Skjorringe, T. & Morgan, E. H. Iron trafficking inside the brain. *J. Neurochem.* **103**, 1730–1740. https://doi.org/10.1111/j.1471-4159.2007.04976.x (2007).
12. Mills, E., Dong, X. P., Wang, F. & Xu, H. Mechanisms of brain iron transport: insight into neurodegeneration and CNS disorders. *Future Med. Chem.* **2**, 51–64. https://doi.org/10.4155/fmc.09.140 (2010).
13. Bien-Ly, N. *et al.* Transferrin receptor (TfR) trafficking determines brain uptake of TfR antibody affinity variants. *J. Exp. Med.* **211**, 233–244. https://doi.org/10.1084/jem.20131660 (2014).
14. Ward, R. J., Zucca, F. A., Duyn, J. H., Crichton, R. R. & Zecca, L. The role of iron in brain ageing and neurodegenerative disorders. *Lancet Neurol.* **13**, 1045–1060. https://doi.org/10.1016/s1474-4422(14)70117-6 (2014).
15. Vela, D. Hepcidin, an emerging and important player in brain iron homeostasis. *J. Transl. Med.* **16**, 25. https://doi.org/10.1186/s12967-018-1399-5 (2018).
16. Bulet, P., Stocklin, R. & Menin, L. Anti-microbial peptides: from invertebrates to vertebrates. *Immunol. Rev.* **198**, 169–184. https://doi.org/10.1111/j.0105-2896.2004.0124.x (2004).
17. Zechel, S., Huber-Wittmer, K. & von Bohlen und Halbach, O. Distribution of the iron-regulating protein hepcidin in the murine central nervous system. *J. Neurosci. Res.* **84**, 790–800. https://doi.org/10.1002/jnr.20991 (2006).
18. Pellegrino, R. M. *et al.* Transferrin receptor 2 dependent alterations of brain iron metabolism affect anxiety circuits in the mouse. *Sci. Rep.* **6**, 30725. https://doi.org/10.1038/srep30725 (2016).
19. Almutairi, M. M., Gong, C., Xu, Y. G., Chang, Y. & Shi, H. Factors controlling permeability of the blood-brain barrier. *Cell. Mol. Life Sci* **73**, 57–77. https://doi.org/10.1007/s00018-015-2050-8 (2016).
20. Farrall, A. J. & Wardlaw, J. M. Blood-brain barrier: ageing and microvascular disease–systematic review and meta-analysis. *Neurobiol. Aging* **30**, 337–352. https://doi.org/10.1016/j.neurobiolaging.2007.07.015 (2009).
21. Salmina, A. B. *et al.* Blood-brain barrier breakdown in stress and neurodegeneration: biochemical mechanisms and new models for translational research. *Biochem. Biokhimiia* **86**, 746–760. https://doi.org/10.1134/s0006297921060122 (2021).
22. Maiuolo, J. *et al.* The "Frail" brain blood barrier in neurodegenerative diseases: role of early disruption of endothelial cell-to-cell connections. *Int. J. Mol. Sci.* https://doi.org/10.3390/ijms19092693 (2018).
23. Jang, S. *et al.* Serum amyloid A1 is involved in amyloid plaque aggregation and memory decline in amyloid beta abundant condition. *Transgenic Res.* **28**, 499–508. https://doi.org/10.1007/s11248-019-00166-x (2019).
24. Jiang, Z., Wang, J., Liu, C., Wang, X. & Pan, J. Hyperoside alleviated N-acetyl-para-amino-phenol-induced acute hepatic injury via Nrf2 activation. *Int. J. Clin. Exp. Pathol.* **12**, 64–76 (2019).
25. O'Callaghan, J. P. & Sriram, K. Glial fibrillary acidic protein and related glial proteins as biomarkers of neurotoxicity. *Expert Opin. Drug Saf.* **4**, 433–442. https://doi.org/10.1517/14740338.4.3.433 (2005).
26. Block, M. L. & Hong, J. S. Microglia and inflammation-mediated neurodegeneration: multiple triggers with a common mechanism. *Prog. Neurobiol.* **76**, 77–98. https://doi.org/10.1016/j.pneurobio.2005.06.004 (2005).
27. Glass, C. K., Saijo, K., Winner, B., Marchetto, M. C. & Gage, F. H. Mechanisms underlying inflammation in neurodegeneration. *Cell* **140**, 918–934. https://doi.org/10.1016/j.cell.2010.02.016 (2010).
28. Hirsch, E. C. & Hunot, S. Neuroinflammation in Parkinson's disease: a target for neuroprotection?. *Lancet Neurol.* **8**, 382–397. https://doi.org/10.1016/S1474-4422(09)70062-6 (2009).
29. Lier, J. *et al.* Loss of IBA1-Expression in brains from individuals with obesity and hepatic dysfunction. *Brain Res.* **1710**, 220–229. https://doi.org/10.1016/j.brainres.2019.01.006 (2019).
30. Zecca, L., Youdim, M. B., Riederer, P., Connor, J. R. & Crichton, R. R. Iron, brain ageing and neurodegenerative disorders. *Nat. Rev. Neurosci.* **5**, 863–873. https://doi.org/10.1038/nrn1537 (2004).
31. Rouault, T. A. Iron metabolism in the CNS: implications for neurodegenerative diseases. *Nat. Rev. Neurosci.* **14**, 551–564. https://doi.org/10.1038/nrn3453 (2013).
32. Yamamoto, A. *et al.* Iron (III) induces aggregation of hyperphosphorylated tau and its reduction to iron (II) reverses the aggregation: implications in the formation of neurofibrillary tangles of Alzheimer's disease. *J. Neurochem.* **82**, 1137–1147. https://doi.org/10.1046/j.1471-4159.2002.t01-1-01061.x (2002).
33. Liu, Y. & Connor, J. R. Iron and ER stress in neurodegenerative disease. *Biometals* **25**, 837–845. https://doi.org/10.1007/s10534-012-9544-8 (2012).
34. Hong, C. H. *et al.* Anemia and risk of dementia in older adults: findings from the Health ABC study. *Neurology* **81**, 528–533. https://doi.org/10.1212/WNL.0b013e31829e701d (2013).
35. Muckenthaler, M. U., Rivella, S., Hentze, M. W. & Galy, B. A red carpet for iron metabolism. *Cell* **168**, 344–361. https://doi.org/10.1016/j.cell.2016.12.034 (2017).
36. Du, F., Qian, Z. M., Luo, Q., Yung, W. H. & Ke, Y. Hepcidin Suppresses brain iron accumulation by downregulating iron transport proteins in iron-overloaded rats. *Mol. Neurobiol.* **52**, 101–114. https://doi.org/10.1007/s12035-014-8847-x (2015).
37. Moos, T. & Morgan, E. H. The metabolism of neuronal iron and its pathogenic role in neurological disease: review. *Ann. N. Y. Acad. Sci.* **1012**, 14–26. https://doi.org/10.1196/annals.1306.002 (2004).
38. Leitner, D. F. & Connor, J. R. Functional roles of transferrin in the brain. *Biochem. Biophys. Acta.* **393–402**, 2012. https://doi.org/10.1016/j.bbagen.2011.10.016 (1820).

39. Ndayisaba, A., Kaindlstorfer, C. & Wenning, G. K. Iron in neurodegeneration—cause or consequence?. *Front. Neurosci.* **13**, 180. https://doi.org/10.3389/fnins.2019.00180 (2019).
40. Yu, M. H. *et al.* SAA1 increases NOX4/ROS production to promote LPS-induced inflammation in vascular smooth muscle cells through activating p38MAPK/NF-κB pathway. *BMC Mol. Cell Biol.* **20**, 15. https://doi.org/10.1186/s12860-019-0197-0 (2019).
41. Erdembileg, A. *et al.* Attenuated age-impact on systemic inflammatory markers in the presence of a metabolic burden. *PLoS ONE* **10**, e0121947. https://doi.org/10.1371/journal.pone.0121947 (2015).
42. Ke, Z. J. & Gibson, G. E. Selective response of various brain cell types during neurodegeneration induced by mild impairment of oxidative metabolism. *Neurochem. Int.* **45**, 361–369. https://doi.org/10.1016/j.neuint.2003.09.008 (2004).
43. Sato, T., Shapiro, J. S., Chang, H. C., Miller, R. A. & Ardehali, H. Aging is associated with increased brain iron through cortex-derived hepcidin expression. *Elife* https://doi.org/10.7554/eLife.73456 (2022).
44. Dowdle, W. E. *et al.* Selective VPS34 inhibitor blocks autophagy and uncovers a role for NCOA4 in ferritin degradation and iron homeostasis in vivo. *Nat. Cell Biol.* **16**, 1069–1079. https://doi.org/10.1038/ncb3053 (2014).
45. Fujimaki, M. *et al.* Iron supply via NCOA4-mediated ferritin degradation maintains mitochondrial functions. *Mol. Cell. Biol.* https://doi.org/10.1128/mcb.00010-19 (2019).
46. Li, X. *et al.* NCOA4 is regulated by HIF and mediates mobilization of murine hepatic iron stores after blood loss. *Blood* **136**, 2691–2702. https://doi.org/10.1182/blood.2020006321 (2020).
47. Kress, G. J., Dineley, K. E. & Reynolds, I. J. The relationship between intracellular free iron and cell injury in cultured neurons, astrocytes, and oligodendrocytes. *J. Neurosci. Off. J. Soc. Neurosci.* **22**, 5848–5855. https://doi.org/10.1523/jneurosci.22-14-05848.2002 (2002).
48. Qian, Z. M. & Ke, Y. Hepcidin and its therapeutic potential in neurodegenerative disorders. *Med. Res. Rev.* **40**, 633–653. https://doi.org/10.1002/med.21631 (2020).
49. Kautz, L. *et al.* Identification of erythroferrone as an erythroid regulator of iron metabolism. *Nat. Genet.* **46**, 678–684. https://doi.org/10.1038/ng.2996 (2014).
50. Casu, C. *et al.* Minihepcidins improve ineffective erythropoiesis and splenomegaly in a new mouse model of adult β-thalassemia major. *Haematologica* **105**, 1835–1844. https://doi.org/10.3324/haematol.2018.212589 (2020).
51. Blanchette, N. L., Manz, D. H., Torti, F. M. & Torti, S. V. Modulation of hepcidin to treat iron deregulation: potential clinical applications. *Expert Rev. Hematol.* **9**, 169–186. https://doi.org/10.1586/17474086.2016.1124757 (2016).
52. Huang, S. N., Ruan, H. Z., Chen, M. Y., Zhou, G. & Qian, Z. M. Aspirin increases ferroportin 1 expression by inhibiting hepcidin via the JAK/STAT3 pathway in interleukin 6-treated PC-12 cells. *Neurosci. Lett.* **662**, 1–5. https://doi.org/10.1016/j.neulet.2017.10.001 (2018).
53. Zhao, Y. *et al.* Nano-liposomes of lycopene reduces ischemic brain damage in rodents by regulating iron metabolism. *Free Radic. Biol. Med.* **124**, 1–11. https://doi.org/10.1016/j.freeradbiomed.2018.05.082 (2018).
54. Livak, K. J. & Schmittgen, T. D. Analysis of relative gene expression data using real-time quantitative PCR and the 2(-Delta Delta C(T)) Method. *Methods* **25**, 402–408. https://doi.org/10.1006/meth.2001.1262 (2001).
55. Boero, M. *et al.* A comparative study of myocardial molecular phenotypes of two tfr2beta null mice: role in ischemia/reperfusion. *BioFactors* **41**, 360–371. https://doi.org/10.1002/biof.1237 (2015).
56. Hage, S. *et al.* Gamma-secretase inhibitor activity of a Pterocarpus erinaceus extract. *Neurodegener. Dis.* **14**, 39–51. https://doi.org/10.1159/000355557 (2014).
57. Stanga, S. *et al.* APP-dependent glial cell line-derived neurotrophic factor gene expression drives neuromuscular junction formation. *FASEB J. Off. Publ. Fed. Am. Soc. Exp. Biol.* **30**, 1696–1711. https://doi.org/10.1096/fj.15-278739 (2016).
58. d'Errico, P. *et al.* Selective vulnerability of spinal and cortical motor neuron subpopulations in delta7 SMA mice. *PLoS ONE* **8**, e82654. https://doi.org/10.1371/journal.pone.0082654 (2013).
59. Roetto, A. *et al.* Comparison of 3 Tfr2-deficient murine models suggests distinct functions for Tfr2-alpha and Tfr2-beta isoforms in different tissues. *Blood* **115**, 3382–3389. https://doi.org/10.1182/blood-2009-09-240960 (2010).
60. Meguro, R. *et al.* Nonheme-iron histochemistry for light and electron microscopy: a historical, theoretical and technical review. *Arch. Histol. Cytol.* **70**, 1–19. https://doi.org/10.1679/aohc.70.1 (2007).

Acknowledgements

Author contributions

M.M. performed research, analyzed data and wrote the paper. G.A. and M.B. performed research and analyzed data. S.S and A.R. designed and performed research, analyzed data and wrote the paper. M.M. and S.S. performed revision. All the authors contributed to the article and approved the submitted version.

Funding

Competing interests

The authors declare no competing interests.

Additional information

Supplementary Information The online version contains supplementary material available at https://doi.org/10.1038/s41598-022-15812-4.

Correspondence and requests for materials should be addressed to S.S. or A.R.

Reprints and permissions information is available at www.nature.com/reprints.

Publisher's note Springer Nature remains neutral with regard to jurisdictional claims in published maps and institutional affiliations.

Activation of the Hepcidin-Ferroportin1 pathway in the brain and astrocytic-neuronal crosstalk to counteract iron dyshomeostasis during aging

Mariarosa Mezzanotte[1], Giorgia Ammirata[1,3], Marina Boido[2], Serena Stanga[2,†,*] and Antonella Roetto[1,†,*]

[1]Department of Clinical and Biological Sciences, University of Turin, Italy;
[2]Neuroscience Institute Cavalieri Ottolenghi, Department of Neuroscience Rita Levi Montalcini, University of Turin, Italy
[3]Current affiliation: Molecular Biotechnology Center Guido Tarone, University of Turin, Italy
[†]These authors contributed equally to this study

*Correspondence: Serena Stanga serena.stanga@unito.it and Antonella Roetto antonella.roetto@unito.it

Supplementary Table 1.
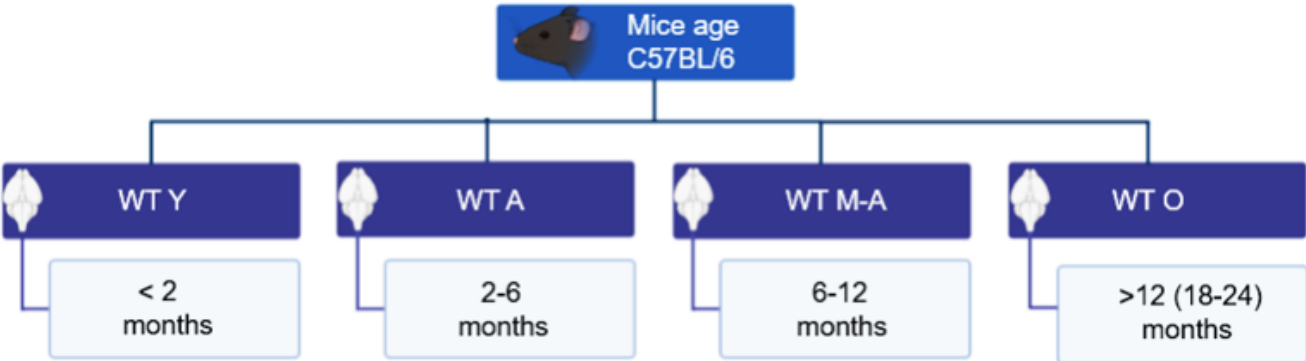
Table 1S: Age and number of mice analyzed in the study

The Jackson Laboratory classification (https://www.jax.org): WT Y, Young (n=5); WT A, Adult (n=7); WT M-A, Middle-Aged (n=5); WT O, Old (n=5).

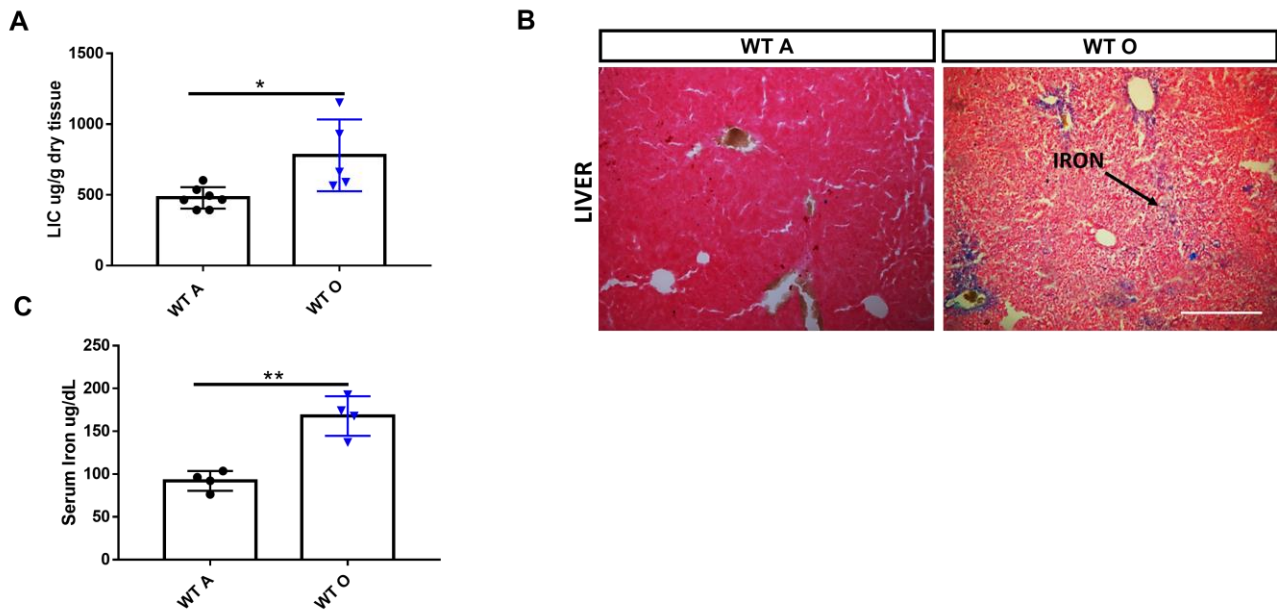**Supplementary Figure 1.**

Figure 1S: Liver and serum iron content.

(**A**) Liver Iron Content (LIC) from Adult and Old mice. (**B**) Sections of mice livers stained with Prussian Blue. Scale bars:10X. (**C**) Serum iron amount from WT A (Adult) and WT O (Old) mice. For serum iron analysis, mice were anaesthetised (ketamine, 100 mg/kg; Ketavet, Bayern, Leverkusen, Germany; xylazine, 5mg/kf; Rompun; Bayer, Milan, Italy) and blood were collected from retro-orbital sinus of mice using a sterile hematocrit tube. Collected blood samples were centrifuged at 3000 g for 10 minutes and serum was taken. Serum iron levels were evaluated by using a commercial kit, Iron Direct Method (Biolabo, Mainz, France), following the manufacturer's instructions. The absorbance was measured at 600 nm via a spectrophotometer. *Statistically significant vs WT A control group *P <0.05; **P <0.01 ***P <0.001 using two-tailed Student's t-test.

Supplementary Table 2.

Genes	Forward Primers (5'-3')	Reverse Primers (5'-3')
Nrf2	ACTTGGAGTTGCCACCG	TTCTCCTGTTCCTTCTGGAG
NCOA4	GCTCCTCAAGTATTGGG	GAAGCCACTCACTCAGAG
Gus-β	GGGACCATCGTCTACAAGACTGA	GCTTGTGTCCTGGACAAAGTAACC

Table 2S: Primers sequences.

The sequences of primers that have been used for amplification are reported in the table. Genes are abbreviated as follows: Nuclear factor erythroid 2-related factor 2 (Nrf2), Nuclear receptor coactivator 4 (NCOA4); β-glucuronidase (Gusb-β). Primers for Nrf2, NCOA4, and Gus-β amplification were designed on the following mRNA sequence: NM_010902.4, NM_019744.4, and NM_010368.2. Primers efficiency was calculated with qRT–PCR (CFX96, BioRad, Hercules, CA, USA) by using serial dilutions of a template cDNAs. Primers showed an efficiency between 90 and 110%. The specificity of each amplicon was evaluated by analyzing the melting curve.

Supplementary List 1 of antibodies used by Western blotting.

1. **<u>Fpn1</u>** polyclonal anti-goat, dilution used: 1:1000.

- Deng Q, Yang S, Sun L, et al. Salmonella effector SpvB aggravates dysregulation of systemic iron metabolism via modulating the hepcidin-ferroportin axis. Gut Microbes. 2021;13(1):1-18. doi:10.1080/19490976.2020.1849996
- Yoshida M, Minagawa S et al. Involvement of cigarette smoke-induced epithelial cell ferroptosis in COPD pathogenesis. Nat Commun. 2019 Jul 17;10(1):3145. doi: 10.1038/s41467-019-10991-7
- Pellegrino RM, Boda E, Montarolo F, Boero M, Mezzanotte M, Saglio G, Buffo A, Roetto A. Transferrin Receptor 2 Dependent Alterations of Brain Iron Metabolism Affect Anxiety Circuits in the Mouse. Sci Rep. 2016 Aug 1;6:30725. doi: 10.1038/srep30725. PMID: 27477597; PMCID: PMC4967901.

2. **<u>ZO1</u>** polyclonal anti-rabbit, dilution used: 1:1000.

- De Tomi E, Campagnari R, Orlandi E, Cardile A, Zanrè V, Menegazzi M, Gomez-Lira M, Gotte G. Upregulation of miR-34a-5p, miR-20a-3p and miR-29a-3p by Onconase in A375 Melanoma Cells Correlates with the Downregulation of Specific Onco-Proteins. Int J Mol Sci2022 Jan 31;23(3):1647. doi: 10.3390/ijms23031647
- HyunA Jo, Dahyun Hwang, Jeong-Keun Kim, Young-Hee Lim. Oxyresveratrol improves tight junction integrity through the PKC and MAPK signaling pathways in Caco-2 cells. Food Chem Toxicol 2017 Oct;108(Pt A):203-213. doi: 10.1016/j.fct.2017.08.002.

3. **<u>NCOA4</u>** polyclonal anti-rabbit, dilution used: 1:1000.

- Kollara A, Ringuette MJ, Brown TJ. Dynamic distribution of nuclear coactivator 4 during mitosis: association with mitotic apparatus and midbodies. PLoS One. 2011;6(7):e22257. doi: 10.1371/journal.pone.0022257.

4. **<u>Ft-L</u>** and **<u>Ft-H</u>** polyclonal antibodies anti-rabbit, dilutions used: 1:1000.

- Pellegrino RM, Boda E, Montarolo F, Boero M, Mezzanotte M, Saglio G, Buffo A, Roetto A. Transferrin Receptor 2 Dependent Alterations of Brain Iron Metabolism Affect Anxiety Circuits in the Mouse. Sci Rep 2016 Aug 1;6:30725. doi: 10.1038/srep30725;

- Santambrogio P, Cozzi A, Levi S, Rovida E, Magni F, Albertini A, Arosio P. Functional and immunological analysis of recombinant mouse H- and L-ferritins from Escherichia coli. Protein Expr Purif 2000 Jun;19(1):212-8. doi: 10.1006/prep.2000.1212.
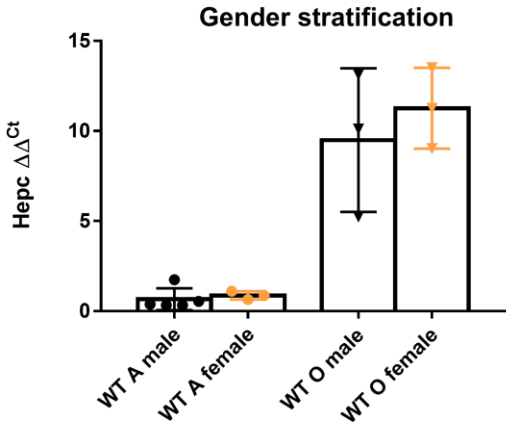
Supplementary Figure 2.

A
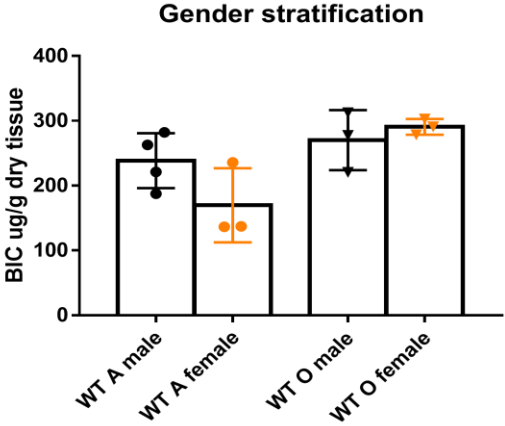
B

Figure 2S: Gender stratification.

(**A**) Brain Iron Content (BIC) parameters and (**B**) Hepc expression: gender stratification between WT A (Adult) *vs* WT O (Old) males and females.
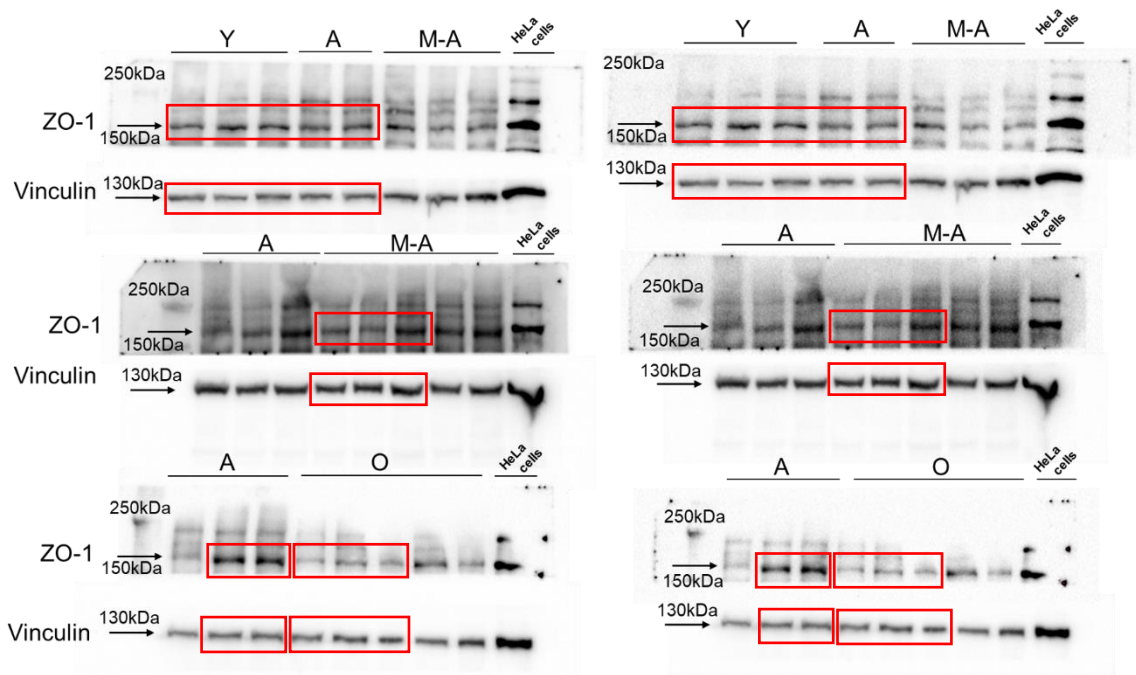
Supplementary Figure 3.

Figure 3S: Zonula occludents-1 protein quantification in the total brain from all age groups.

Full-length western blottings of ZO-1 protein (ZO-1). HeLa cells were used as a positive control. Blots were cut prior to over night hybridization with primary antibodies according to their molecular weight: 195 kDa for ZO-1 and 130 kDa for Vinculin. The regions of the original blots used in main figures are denoted by red boxes. On the right, we reported images with low contrast. Data were normalized on Vinculin amount in the same samples (Image Lab 4.0.1 Software, Bio-Rad, California, USA).
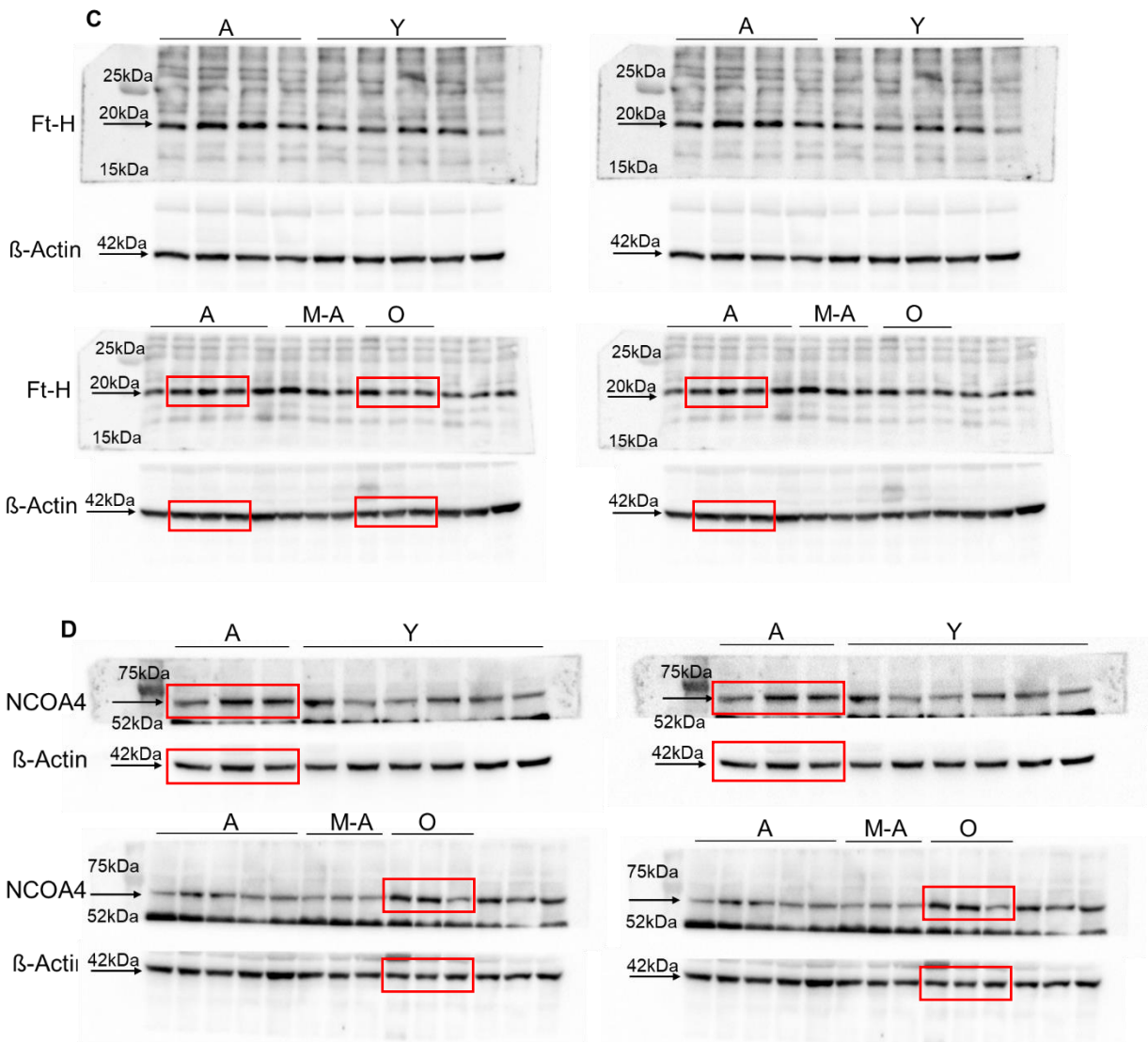
Supplementary Figure 4.
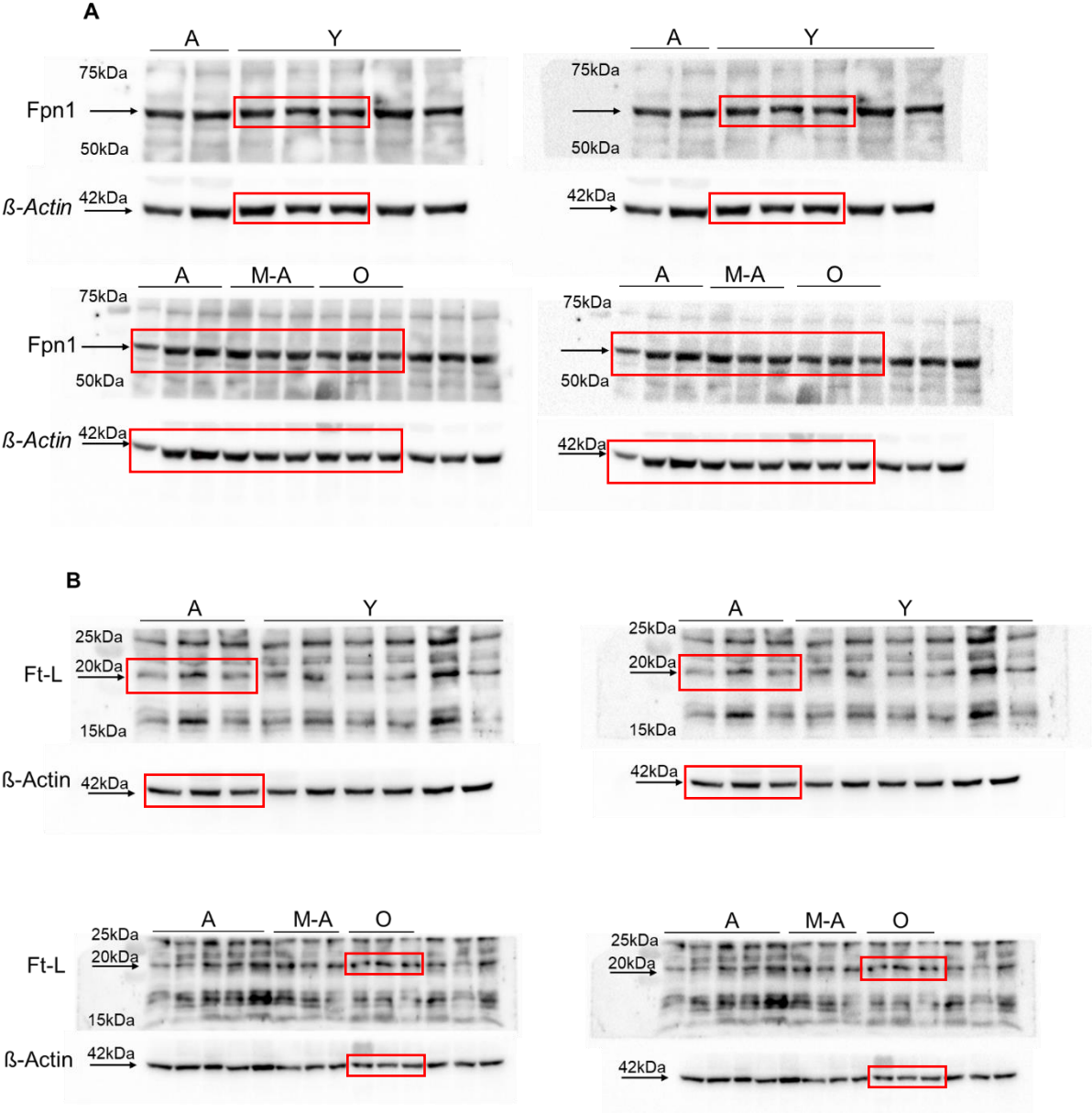
Figure 4S: Iron proteins quantification in the total brain from all age groups.

Full-length western blottings of (**A**) Ferroportin 1 (Fpn1), (**B**) Ferritin-L (Ft-L), (**C**) Ferritin-H (Ft-H) and (**D**) Nuclear receptor coactivator 4 (NCOA4). Data were normalized on the β-Actin amount in the same samples (Image Lab 4.0.1 Software, Bio-Rad, California, USA. Blots were cut prior to over night hybridization with primary antibodies according to their molecular weight: 65 kDa for Fpn1, 19 kDa for Ft-L and Ft-H, 70 kDa for NCOA4 and 42 kDa for β-actin. The regions of the original blots used in the main figures are denoted by red boxes. On the right, we reported images with low contrast.
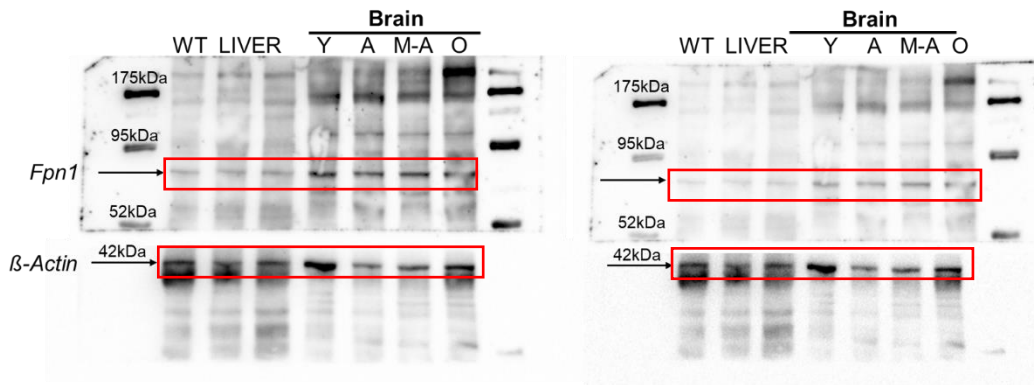
Supplementary Figure 5.

Figure 5S: Ferroportin 1 protein in total liver and brain from all age groups.

Full-length western blottings of Ferroportin 1 (Fpn1). Wild-type mouse livers were used as a positive control. Blots were cut prior to oven nigh hybridization with primary antibodies according to their molecular weight: 65 kDa for Fpn1 and 42 kDa for β-actin. The regions of the original blots used in main figures are denoted by red boxes. On the right, we reported images with low contrast.
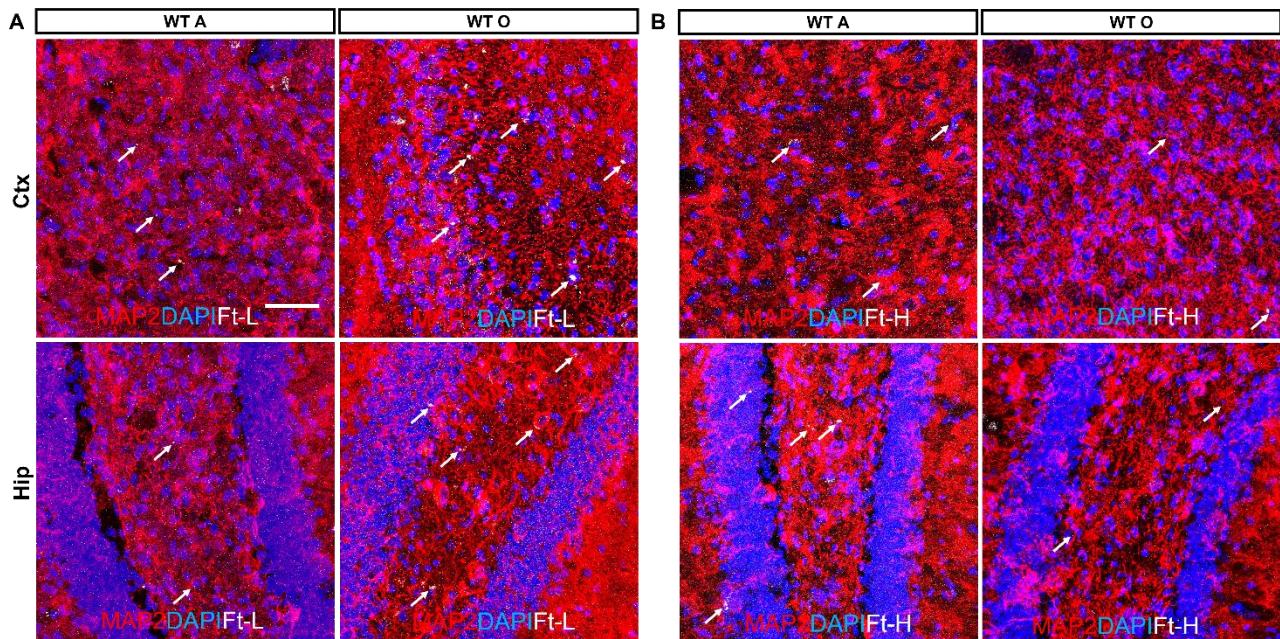
Supplementary Figure 6.

Figure 6S. Ferritin L and Ferritin H proteins cellular allocation in Ctx and Hip.

(**A**) Anti-Ft-L and (**B**) anti-Ft-H in cerebral cortex (Ctx) and hippocampus (Hip) of WT A and WT O mice. Immunofluorescence showing that Ft-L and Ft-H localize both at the level of neuronal soma in the cerebral cortex and hippocampus. To note, also in non-denaturing conditions Ft-H deposits show a reverse trend of expression compared to Ft-L deposits: Ft-H levels are lower in WT A vs WT O; Ft-L levels are higher ın WT O vs WT A. Neuronal cells are marked with anti-MAP2 (red), anti-Ft-L or H antibodies (white) are indicated also by arrows and 4,6-diamidino-2-phenylindole (DAPI) (blue) is used to counterstain cell nuclei in cerebral cortex (Ctx) and hippocampus (Hip). Scale bars: 63X.